Top-Quark Pair Production Close to Threshold
QCD and Electroweak Effects

Johann H. Kühn

I. QCD
(based on EPJ (2009); Kiyo, JK, Moch, Steinhauser, Uwer)

II. Electroweak Corrections
(with Scharf, Uwer)

Karlsruhe Institute of Technology

I) QCD and Threshold Effects

Remember the ILC

Original idea from e^+e^- annihilation

$$\sigma(e^+e^- \to t\bar{t}) \sim \sum_n |\Psi_n(0)|^2 \pi\delta(\sqrt{s} - M_n)$$

for narrow $t\bar{t}$-resonances with masses M_n and “stable” top quarks.

Finite width: $\pi\delta(\sqrt{s} - M_n) \Rightarrow \mathbf{Im}\frac{1}{M_n - i\Gamma_t - \sqrt{s}}$

$$\sum_n \frac{\Psi_n(0)\Psi_n^*(0)}{M_n - i\Gamma_t - \sqrt{s}} = \mathbf{Im}\, G(\vec{r} = 0, \vec{r}' = 0, \sqrt{s} + i\Gamma_t)$$

numerical or perturbative analytical solution of Lippmann-Schwinger equation

$$\left[(E + i\Gamma_t) - \left(-\frac{\nabla^2}{m_t^2} + V(\vec{r}) \right) \right] G(\vec{r}, \vec{r}' = 0, E + i\Gamma_t) = \delta(\vec{r})$$

Greens function G involves "long distances"

($\langle P \rangle \sim 20$ GeV) still in perturbative region

In addition: short distance corrections $\left(1 - \frac{16}{3}\frac{\alpha_s}{\pi} + \ldots\right)$

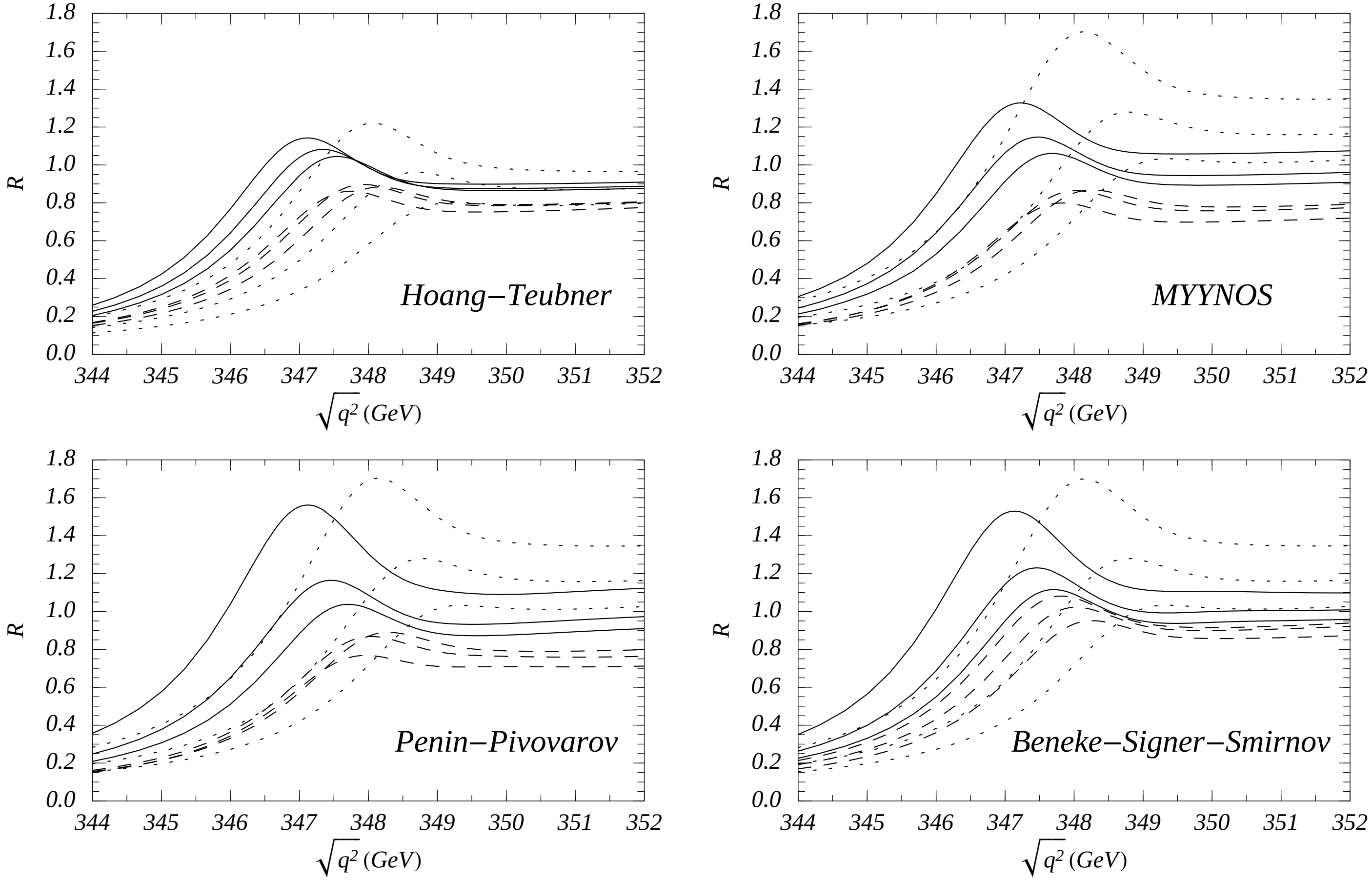

determination of m_t with $\delta m_t \sim 50$ MeV (Linear Collider)

$\Rightarrow$ important impact on stability of vacuum in the SM.

Hadron Colliders

Tevatron, LHC: $\delta m_t \sim 1$ GeV

systematics limited:

Kinematical reconstruction from decay products of top quarks (color triplet)

“Monte Carlo” defintion ($\sim$ close to pole mass) fundamental processes:

$$q\bar{q} \quad \rightarrow \quad g^* \quad \rightarrow \quad t + \bar{t} \quad \text{(Tevatron)}$$

$\nwarrow$ color octet (8_s) $\nearrow$

$$gg \rightarrow t + \bar{t}$$

$$8 \otimes 8 = \boxed{1_s \oplus 8_s} \oplus 8_a \oplus 10_a \oplus \overline{10}_a \oplus 27_s$$

$$3 \otimes \bar{3} = \boxed{1_s \oplus 8_s}$$

QCD potential

$$\widetilde{V}_C^{[1,8]}(\vec{q}) \quad = \quad -\frac{4\pi\alpha_s(\mu_r)\, C^{[1,8]}}{\vec{q}^{\,2}} \left[1 + \frac{\alpha_s(\mu_r)}{4\pi}\left(\beta_0 \ln\frac{\mu_r^2}{\vec{q}^{\,2}} + a_1\right) + \ldots\right],$$

with $C^{[1]} = C_F = 4/3$ and $C^{[8]} = C_F - C_A/2 = -1/6$, and $a_1 = (31/9)\,C_A - (20/9)\,T_F\, n_f$

singlet: attractive

octet: repulsive

$t\bar{t}$ bound states?

$\Gamma_t \approx 1.36$ GeV; Rydberg constant $(C^{[1]}\alpha_s)^2 \, \frac{m_t}{4} \approx 1.5$ GeV

singlet $\Rightarrow$ enhancement around 1S peak

octet $\Rightarrow$ suppression

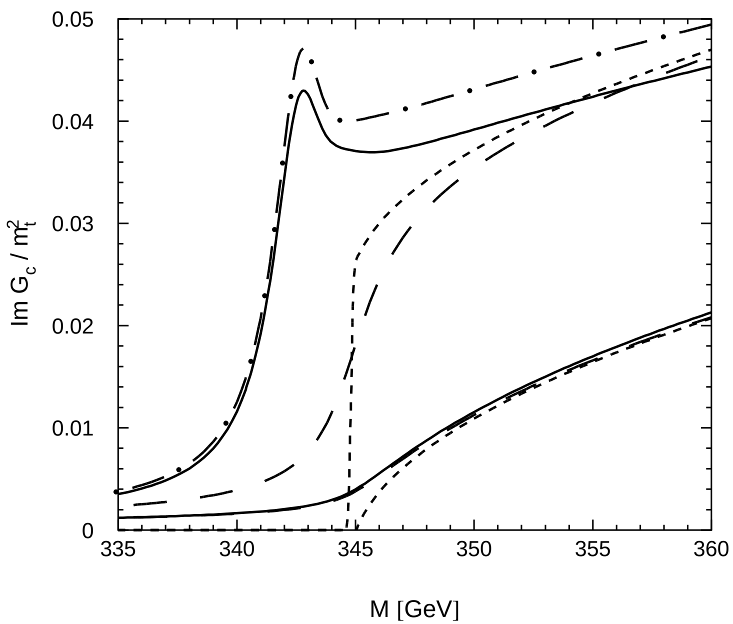

Imaginary part of the Green's functions for the color singlet (upper solid line) and color octet (lower solid line) cases as functions of top quark invariant mass. For comparison, also the expansions of G in fixed order up to $O(\alpha_s)$ with (dashed) and without (dotted line) Γ_t are plotted. The imaginary part of the NNLO Green's function for the color-singlet case is shown as dash-dotted line.

Production cross section close to threshold

partonic cross section

Born: $i + j \to t + \bar{t}$

QCD-corrections:

$i + j \to t + \bar{t}(+X)$
(e.g. $q + \bar{q} \to t + \bar{t} + g$ etc)

$$M \frac{d\hat{\sigma}_{ij\to t\bar{t}}}{dM}(\hat{s}, M^2, \mu_f^2) = F_{ij\to t\bar{t}}(\hat{s}, M^2, \mu_f^2) \frac{1}{m_t^2} \operatorname{Im} G^{[1,8]}(M + i\Gamma_t),$$

Perturbative NLO evaluation:

$$F_{ij\to t\bar{t}}(\hat{s}, M^2, \mu_f^2) = \mathcal{N}_{ij\to t\bar{t}} \frac{\pi^2 \alpha_s^2(\mu_r)}{3\hat{s}} \left(1 + \frac{\alpha_s(\mu_r)}{\pi} C_h\right) \times \left[\delta_{ij\to t\bar{t}} \delta(1-z) + \frac{\alpha_s(\mu_r)}{\pi} \left(\mathcal{A}_c(z) + \mathcal{A}_{nc}(z)\right)\right].$$

restrict to S-waves: ${}^1S_0^{[1]},\ {}^1S_0^{[8]},\ {}^3S_1^{[1]},\ {}^3S_1^{[8]}$
spin singlet and triplet, color singlet and octet
(result for spin and color singlet: JK+Mirkes 1993)

- $\mathcal{N}_{ij}$: normalization
- $\mathcal{C}_h$: hard virtual corrections
- $\mathcal{A}_c$: collinear parton splitting (involves splitting functions)
- $\mathcal{A}_{nc}$: non-collinear real emission

example ($t\bar{t}$ in spin singlet & color singlet configuration)

$$\mathcal{C}_h[gg \to {}^1S_0^{[1]}] = \frac{\beta_0}{2}\ln\left(\frac{\mu_r^2}{M^2}\right) + C_F\left(\frac{\pi^2}{4} - 5\right) + C_A\left(1 + \frac{\pi^2}{12}\right),$$

$$\mathcal{A}_c[gg \to {}^1S_0^{[1,8]}] = (1-z)P_{gg}(z)\left\{2\left[\frac{\ln(1-z)}{1-z}\right]_+ + \left[\frac{1}{1-z}\right]_+ \ln\left(\frac{M^2}{z\mu_f^2}\right)\right\} - \frac{\beta_0}{2}\delta(1-z)\ln\left(\frac{\mu_f^2}{M^2}\right),$$

$$\mathcal{A}_c[gq \to {}^1S_0^{[1,8]}] = \frac{1}{2}P_{gq}(z)\ln\left(\frac{M^2(1-z)^2}{z\mu_f^2}\right) + \frac{C_F}{2}z,$$

$$\mathcal{A}_{nc}[gg \to {}^1S_0^{[1]}] = \frac{-C_A}{6z(1-z)^2(1+z)^3}\Big[12 + 11z^2 + 24z^3 - 21z^4 - 24z^5 + 9z^6 - 11z^8 + 12\left(-1 + 5z^2 + 2z^3 + z^4 + 3z^6 + 2z^7\right)\ln z\Big],$$

$$\mathcal{A}_{nc}[q\bar{q} \to {}^1S_0^{[1]}] = \frac{32C_F}{3N_c^2}z(1-z)$$

similarly for ${}^1S_0^{[8]}$, also contributions from gq, $q\bar{q}$

Results

leading subprocesses: $gg \to {}^1S_0^{[1,8]}$ and $q\bar{q} \to {}^3S_0^{[8]}$

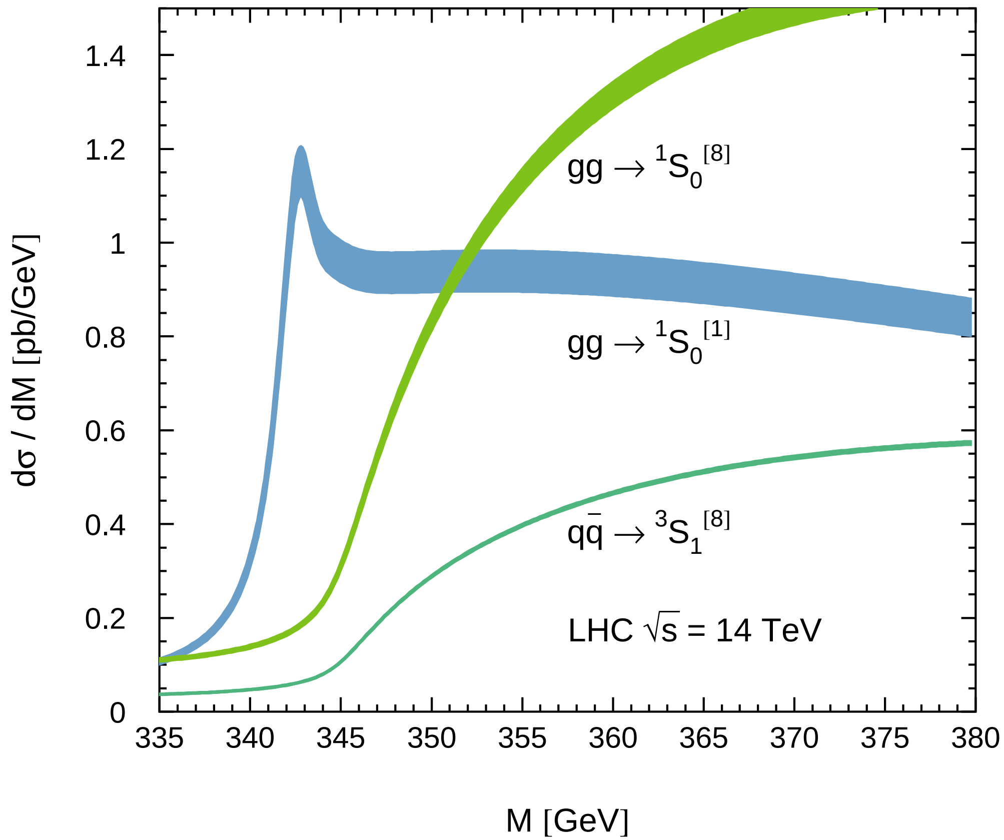

octet: suppressed (repulsive potential ⇒ Greens function)
enhanced (color degrees of freedom)

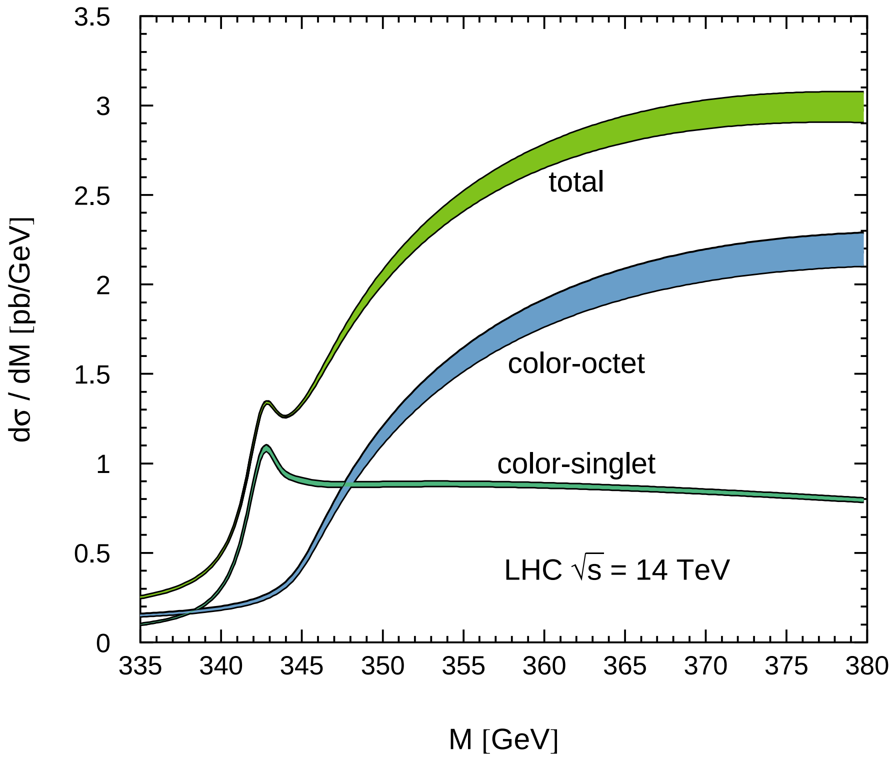

all production channels

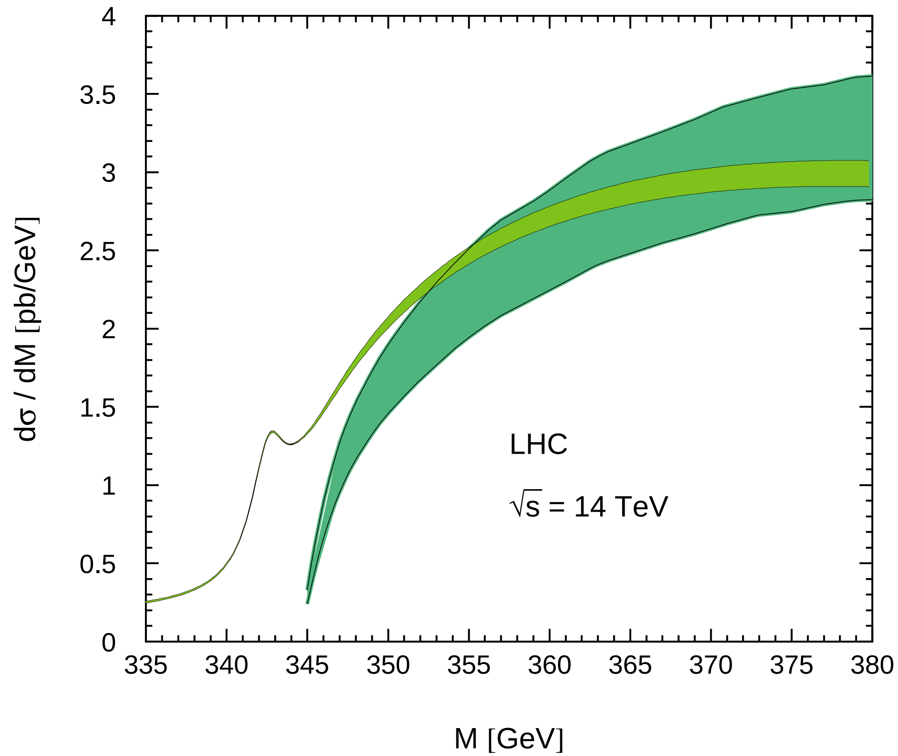

boundstate result vs NLO

(continuum pQCD)

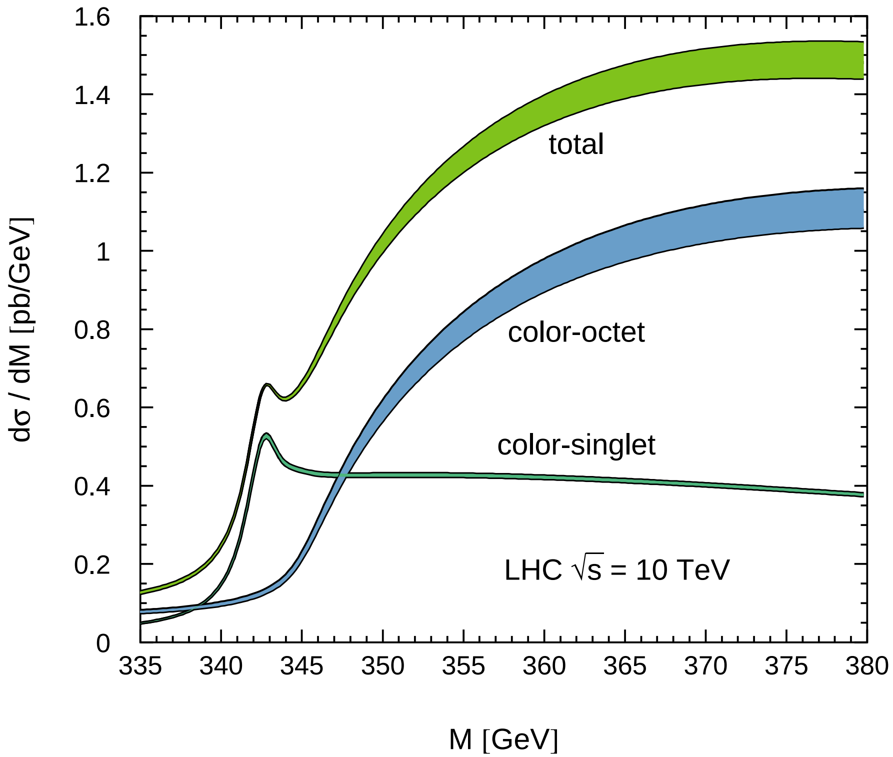

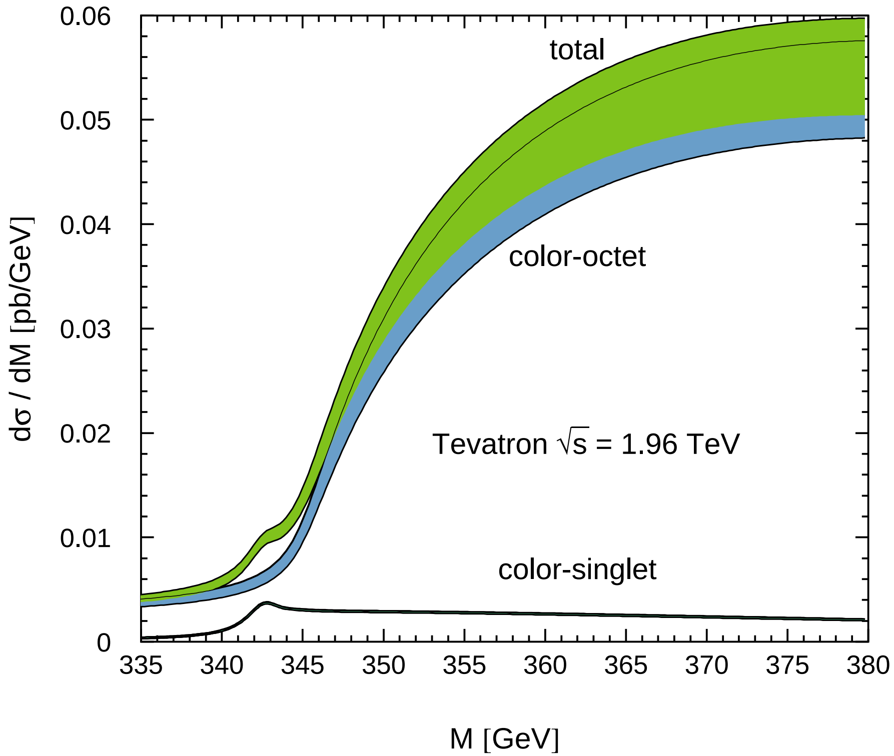

LHC (10 TeV)

Tevatron (1.96 TeV)

small gg-luminosity

SUMMARY on QCD

differential distribution $\frac{d\sigma}{dM}$

carries important information on $t - \bar{t} -$dynamics

threshold enhancement $\sim$ 10 pb

[small compared to σ_{tot} $\sim$ 200 pb (8 TeV)
$\sim$ 800 pb (14 TeV)]

studies of $\frac{d\sigma}{dM}$ close to threshold might exhibit structure similar to those at e^+e^- colliders

$\Rightarrow$ mass of $t\bar{t}$ bound state

Impact of weak corrections?

II) Electroweak Corrections

I. Results at Partonic Level

$q\bar{q} \to t\bar{t}$:

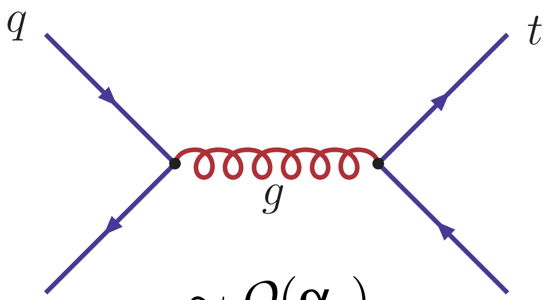

$\sim \mathcal{O}(\alpha_s)$

no
interference
with

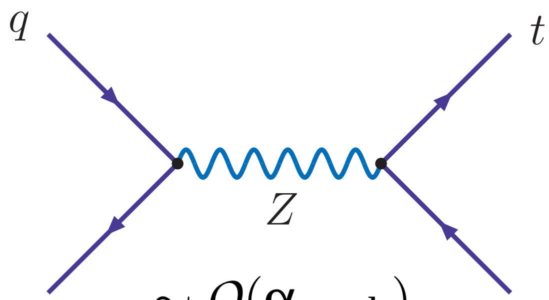

$\sim \mathcal{O}(\alpha_{weak})$

$gg \to t\bar{t}$:

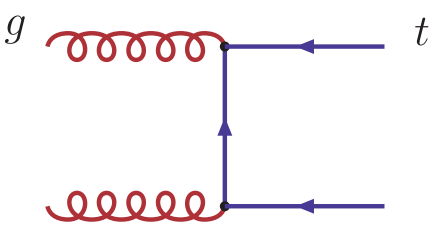

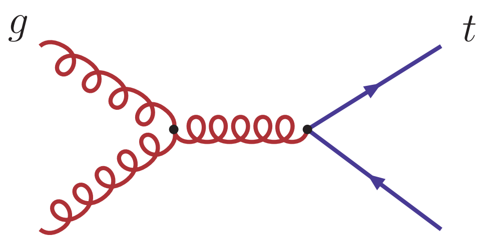

$\sim \mathcal{O}(\alpha_s)$

$O(\alpha_s^2 \alpha_{\text{weak}})$ weak corrections $(q\bar{q} \to t\bar{t})$

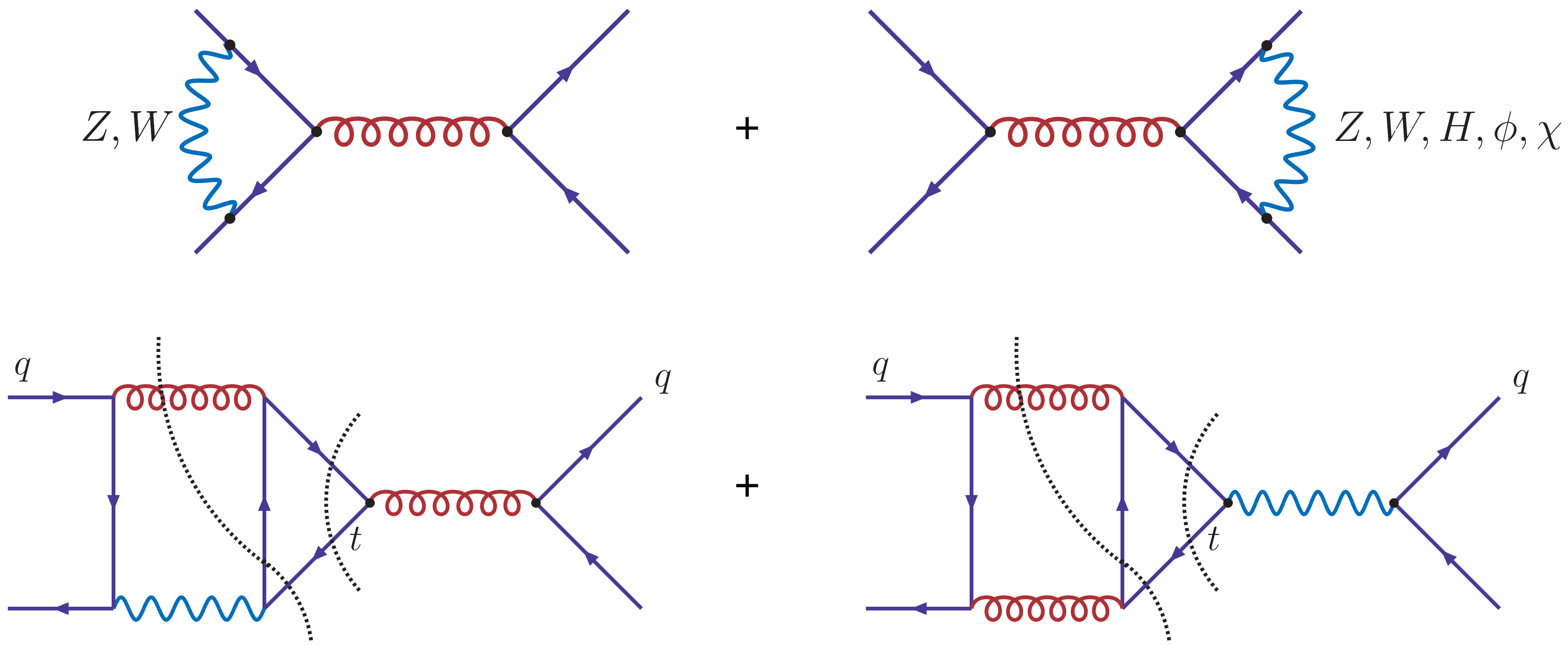

cuts of second group individually IR-divergent

$O(\alpha_s^2\alpha_{\mathrm{weak}})$ weak corrections $(gg \to t\bar{t})$

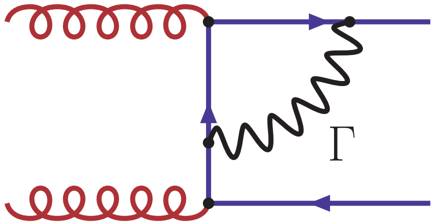

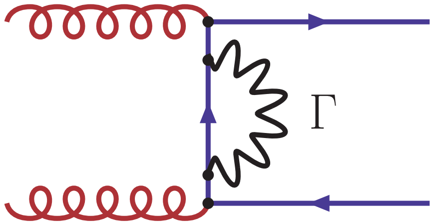

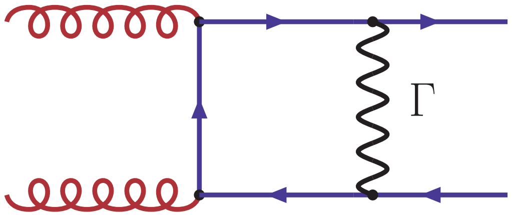

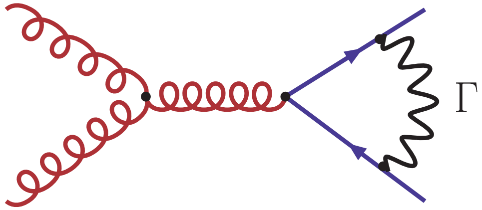

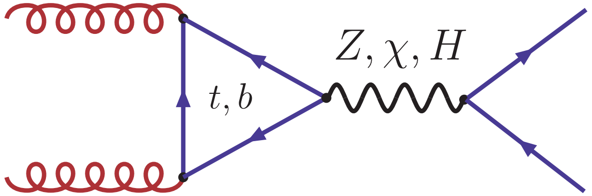

- analytical & numerical results available
  (earlier partial results by Beenakker *et al.*, some disagreements)
  independent evaluation by Bernreuther & Fücker

- $(\text{box contribution})_{\text{up-quark}} = -(\text{box contribution})_{\text{down-quark}}$
  $\Rightarrow$ suppression

- box contribution moderately $\hat{s}$-dependent

- strong increase of negative corrections with $\hat{s}$

- sizable M_{h}-dependence, large effect close to threshold

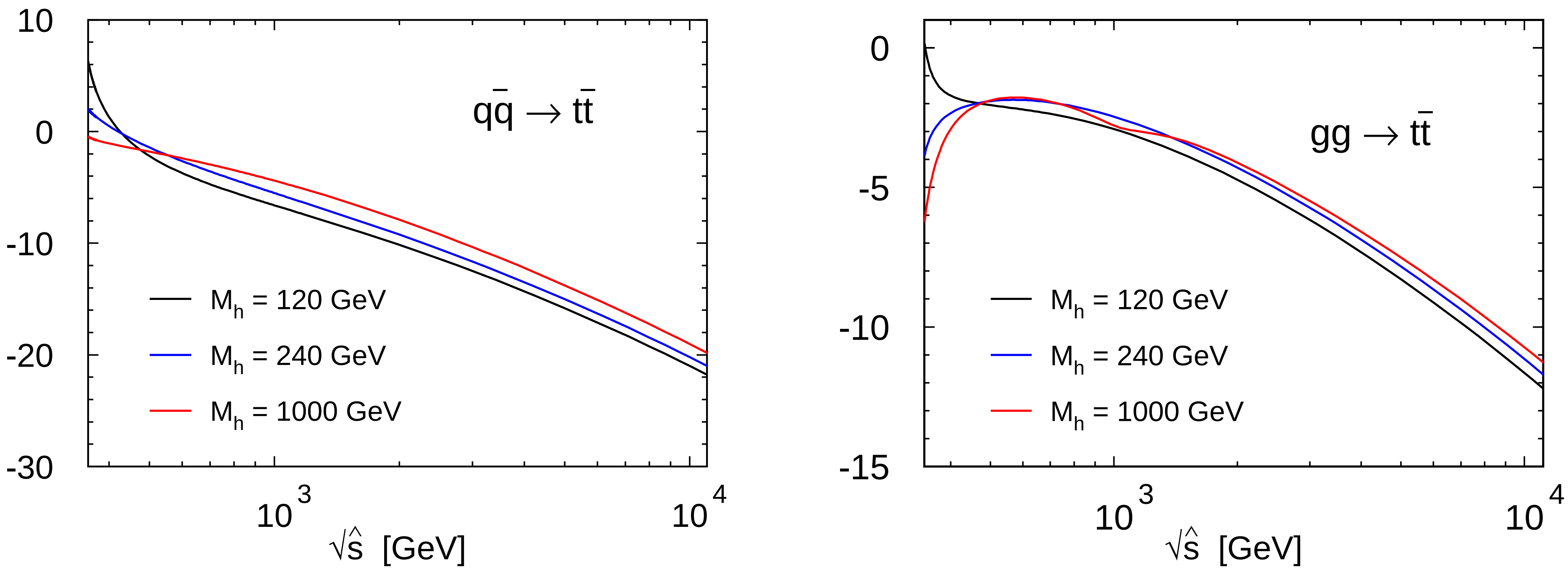

- sizable negative corrections for large $E_{cm} = M(t\bar{t}) \Rightarrow$ Sudakov logarithms

- weak charges in initial and final state $\Rightarrow$ factor two enhanced corrections

- significant dependence on m_H close to threshold

II. Tevatron and LHC

Small effects for total cross section

(dominated by $\sqrt{\hat{s}} \sim 360\text{-}380$ GeV)

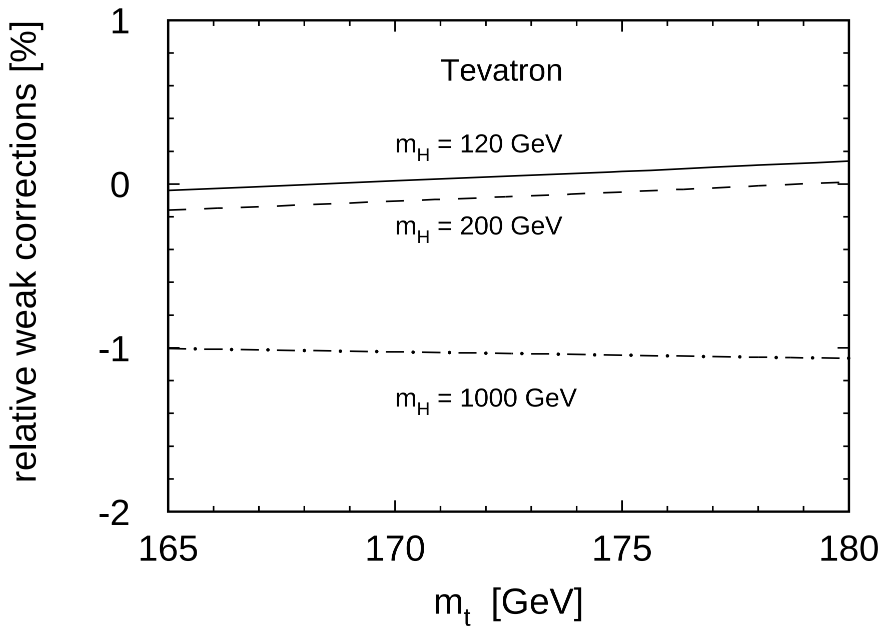

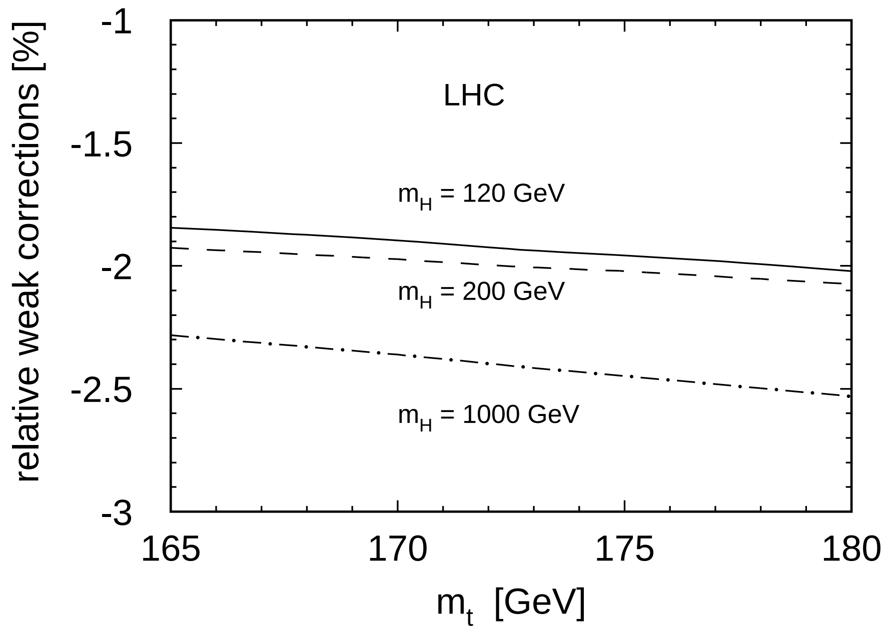

differential distributions

composition: $q\bar{q}$ vs gg

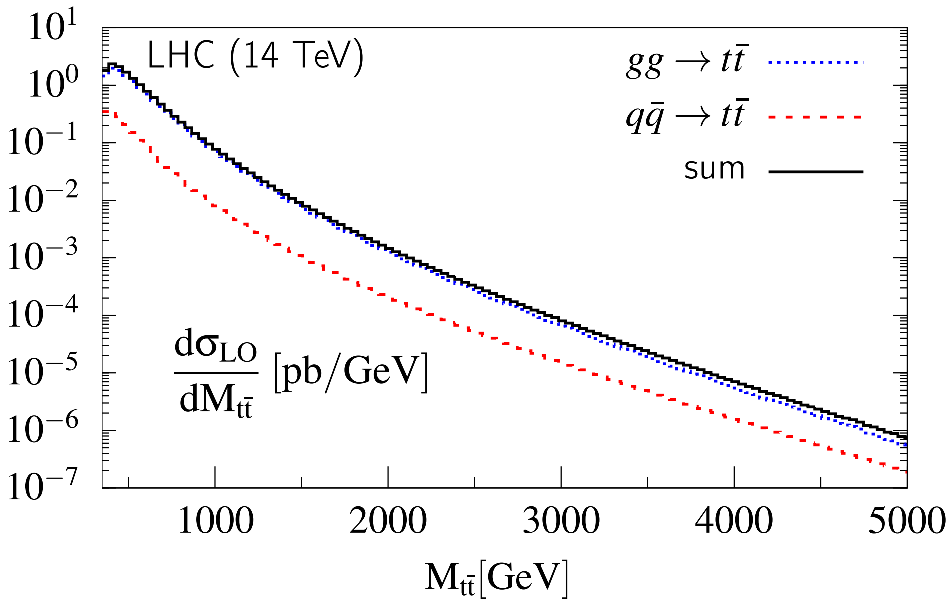

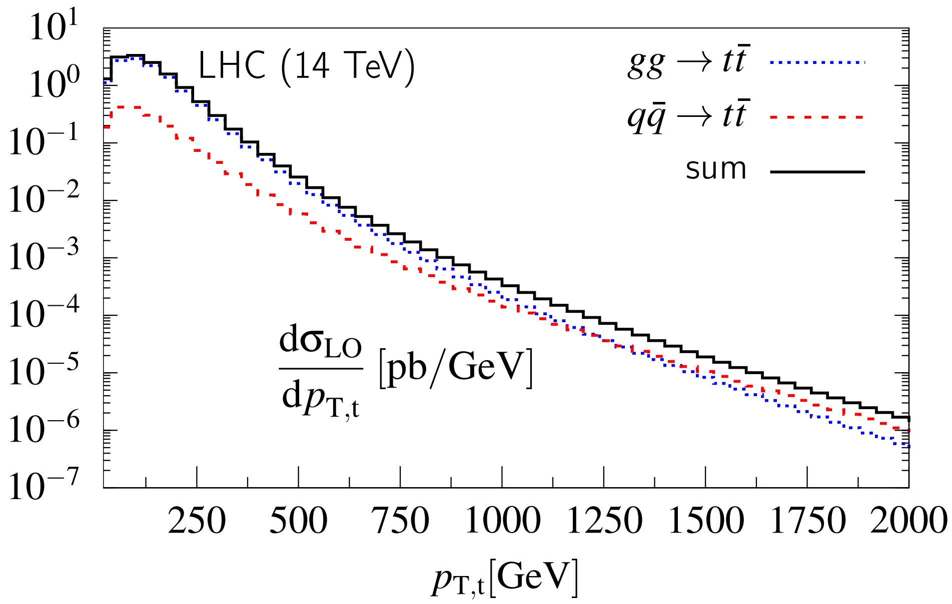

large p_t: dominated by $q\bar{q}$ annihilation

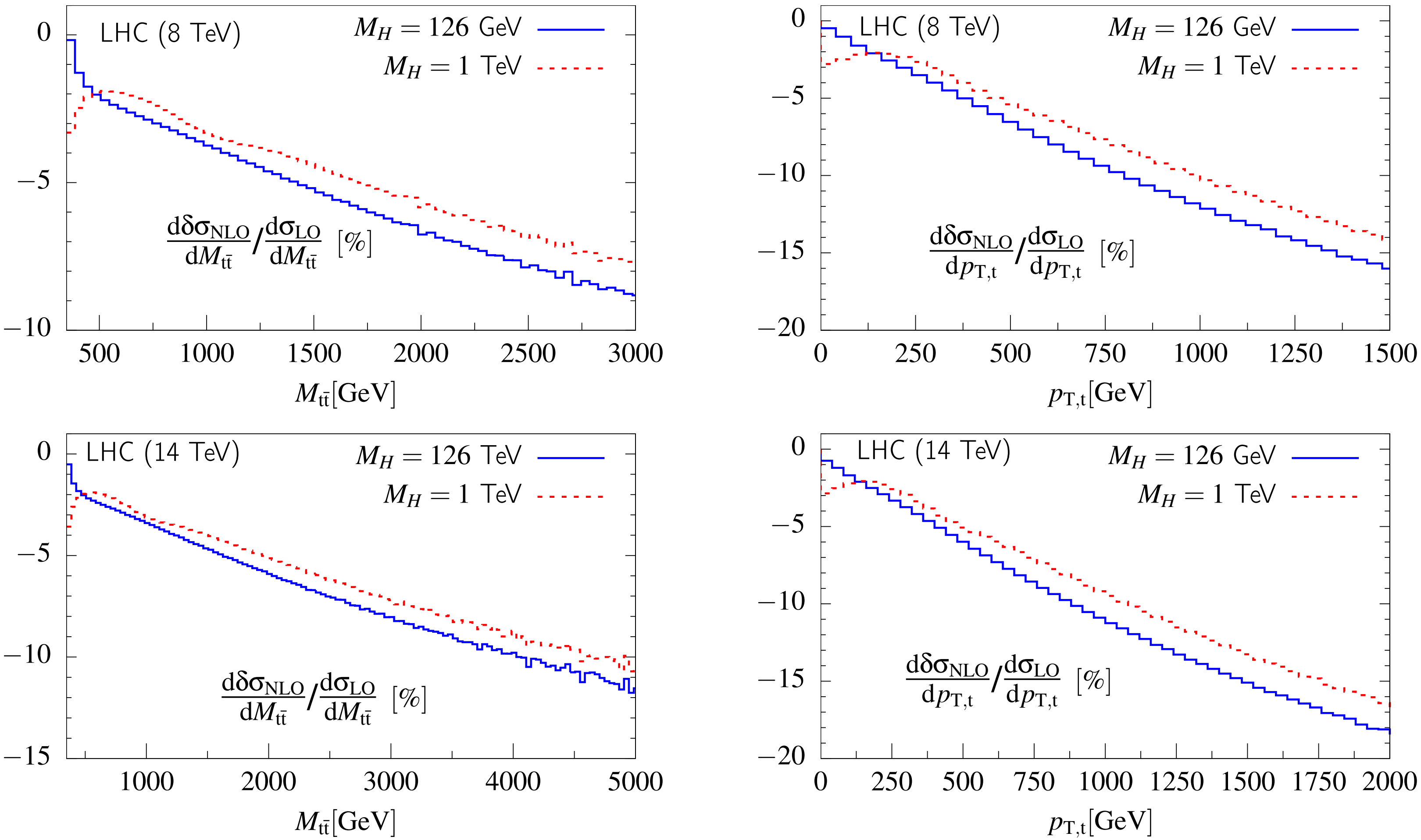

Relative weak corrections for the invariant $t\bar{t}$ mass (left) and transverse momentum (right) distribution for LHC8 (upper) and LHC14 (lower plots) and for Higgs masses of 126 GeV and 1 TeV.

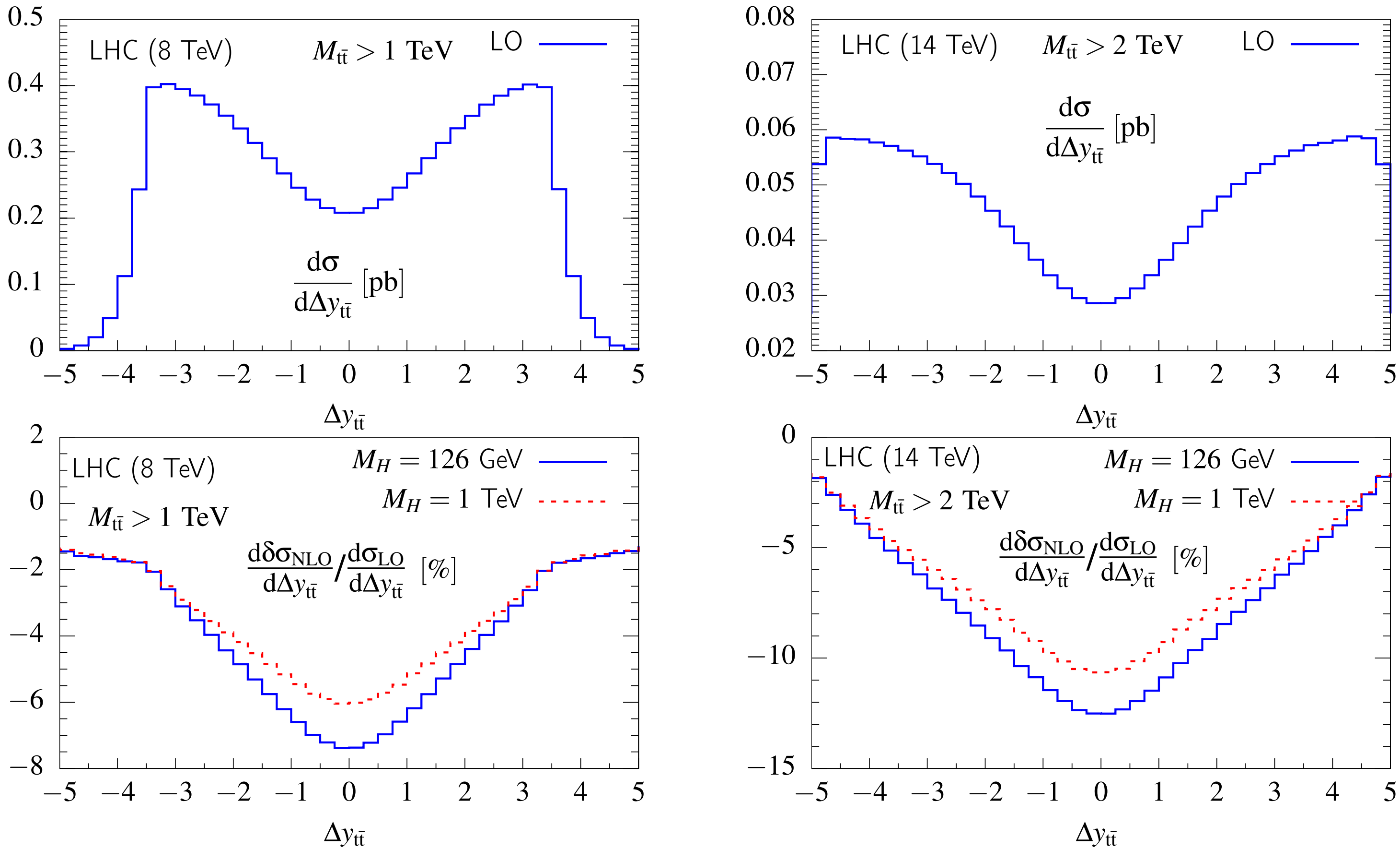

Rapidity distributions with invariant mass cuts at leading order (upper plots) and relative weak corrections to these distributions (lower plots) for LHC8 (left) and LHC14 (right).

rapidity difference $\hat{=}$ scattering angle
distortions of order 10%
(large corrections for $\Delta y_{t\bar{t}} = 0$! $\hat{=}$ scattering at 90°)

III. Higgs exchange and Yukawa potential

$$V_Y(r) = -\kappa \frac{1}{r} e^{-r/r_Y} \quad \text{with} \quad \kappa = \frac{g_Y^2}{4\pi} = \frac{\sqrt{2} G_F M_t^2}{4\pi} \approx 0.0337 \quad \text{and} \quad r_Y = 1/M_H$$

short range potential relative to bound state

range of potential $= r_Y = 1/M_H$

size of bound state $= r_{Bohr} = \frac{4}{3}\alpha_s \frac{M_t}{2}$

$\frac{r_Y}{r_{Bohr}} \approx \frac{1}{6}$

correction factor $\left(1 + \kappa \frac{M_t}{M_H}\right) \approx (1 + 0.05)$

rapid variation below $M_{t\bar{t}} =$ 400 GeV

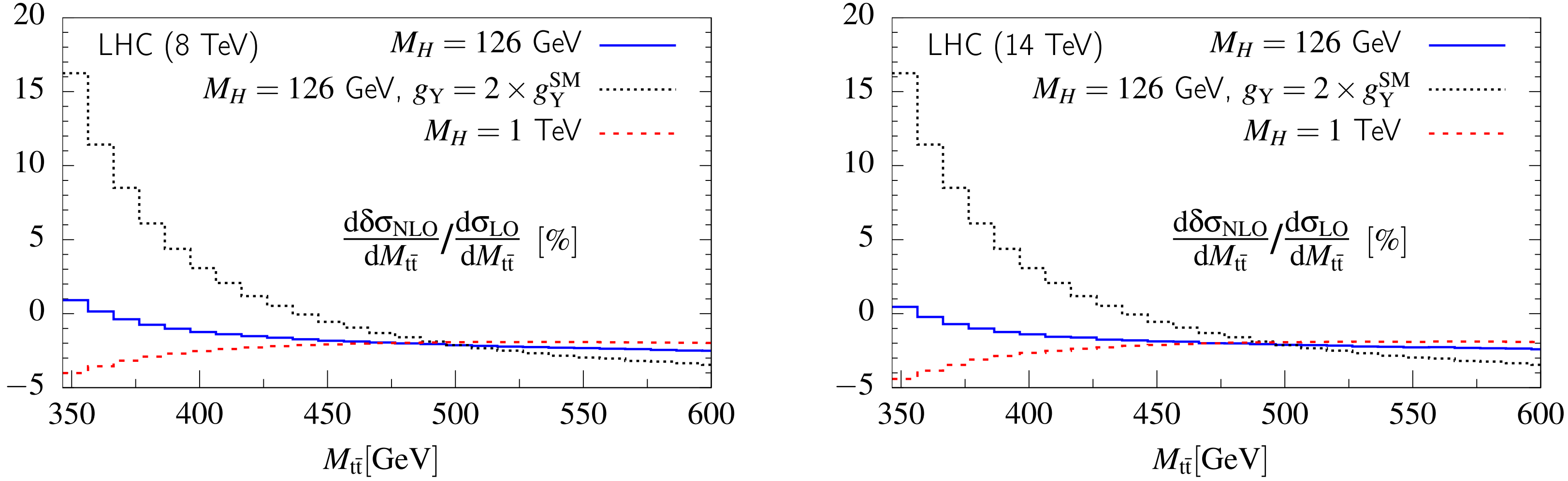

Relative weak corrections for the mass distribution in the framework of the SM assuming $M_H = 126$ GeV (solid blue curve) and 1000 GeV (dashed red curve), and for the case of an enhanced Yukawa coupling $g_Y = 2g_Y^{SM}$ with $M_H = 126$ GeV (dotted black curve). The two plots represent LHC8 and LHC14.

more pronounced for Tevatron!

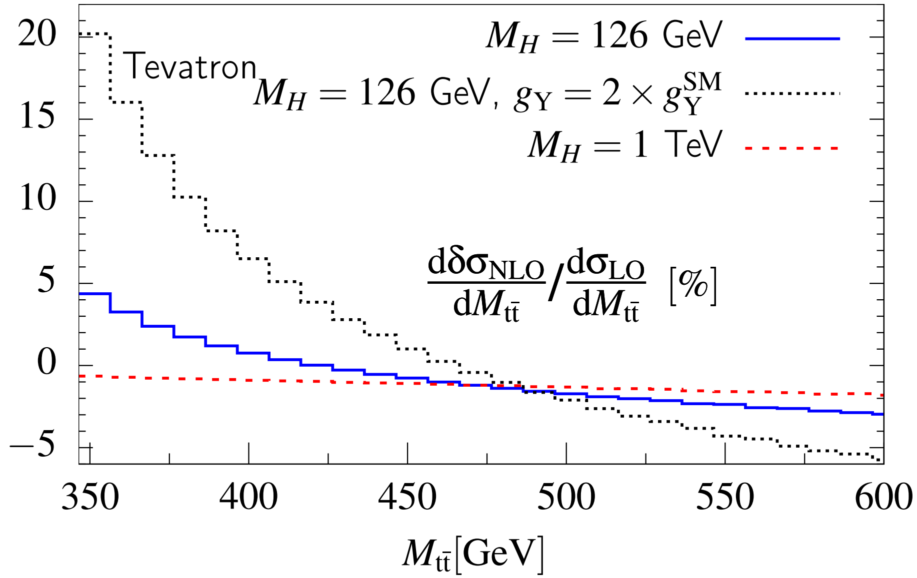

$\Rightarrow$ non-trivial limit on Yukawa coupling within reach! ($g_Y < 2g_{SM}$?)

$\Rightarrow$ detailed theoretical understanding of threshold region required!

SUMMARY

LHC $=$ Top Quark Factory (Millions of top quarks)

extreme regions will be explored:

- large p_T of $O(1\text{TeV})$
  $\Rightarrow$ large weak corrections

- close to threshold
  $\Rightarrow$ complicated dynamics, remnant of $t\bar{t}$ resonances;
  $\Rightarrow$ QCD and Yukawa potential

- NLO results available for strong and electroweak interactions